Draft of new SC section

Sean Bittner

November 4, 2020

# 1 Identifying neural mechanisms of flexible task switching

In a rapid task switching experiment [1], rats were explicitly cued on each trial to either orient towards a visual stimulus in the Pro (P) task or orient away from a visual stimulus in the Anti (A) task (Fig. 1a). Neural recordings in the midbrain superior colliculus (SC) exhibited two populations of neurons that simultaneously represented both task context (Pro or Anti) and motor response (contralateral or ipsilateral to the recorded side): the Pro/Contra and Anti/Ipsi neurons [2]. Duan et al. proposed a model of SC that, like the V1 model analyzed in the previous section, is a four-population dynamical system. We analyzed this model, where the neuron-type populations are functionally-defined as the Pro- and Anti-populations in each hemisphere (left (L) and right (R)), their connectivity is parameterized geometrically (Fig. 1B). The input-output function of this model is chosen such that the population responses $\mathbf{x} = [x_{LP}, x_{LA}, x_{RP}, x_{RA}]^\top$ are bounded from 0 to 1 as a function $f$ of a dynamically evolving internal variable $\mathbf{u}$. The dynamics evolve with timescale $\tau = 0.09$ governed by connectivity weights $W$

$$\begin{aligned} \tau \frac{d\mathbf{u}}{dt} &= -\mathbf{u} + W\mathbf{x} + \mathbf{h} + \epsilon d\mathbf{B} \\ \mathbf{x} &= f(\mathbf{u}) \end{aligned} \tag{1}$$

with white noise of variance $\epsilon^2 = 0.2^2$. The input $\mathbf{h}$ is comprised of a cue-dependent input to the Pro or Anti populations, a stimulus orientation input to either the Left or Right populations, and a choice-period input to the entire network (see Section 2). Here, we use EPI to determine the changes in network connectivity $\mathbf{z} = [sW, vW, dW, hW]^\top$ resulting in execution of rapid task switching behavior.

We define rapid task switching behavior as accurate execution of each task. Inferred models should not exhibit fully random responses (50%), or perfect performance (100%), since perfection is never attained by even the best trained rats. We formulate rapid task switching as an emergent property by stipulating that the average accuracy in the Pro task $p_P(\mathbf{x}, \mathbf{z})$ and Anti task $p_A(\mathbf{x}, \mathbf{z})$ be 75% with variance $5\%^2$.

$$\begin{aligned} \mathcal{X} \quad : \quad \mathbb{E}_{\mathbf{z}} \begin{bmatrix} p_P(\mathbf{x};\mathbf{z}) \\ p_A(\mathbf{x};\mathbf{z}) \end{bmatrix} &= \begin{bmatrix} 75\% \\ 75\% \end{bmatrix} \\ \mathrm{Var}_{\mathbf{z}} \begin{bmatrix} p_P(\mathbf{x};\mathbf{z}) \\ p_A(\mathbf{x};\mathbf{z}) \end{bmatrix} &= \begin{bmatrix} 5\%^2 \\ 5\%^2 \end{bmatrix} \end{aligned} \tag{2}$$

A variance of 5% performance in each task will confer a posterior producing performances ranging from about $65\% - 85\%$, allowing us to examine the properties of connectivity that yield better performance.

We ran EPI to obtain SC model connectivity parameters $z$ producing rapid task switching (Fig. 1C). To make sense of this inferred distribution, we followed the approach of Duan et al. by decomposing the connectivity matrix $W = V\Lambda V^{-1}$ in such a way (the Schur decomposition) that the basis vectors $v_i$ are the same for all $W$ (Fig. 2A). These basis vectors have intuitive roles in processing for this task, and are accordingly named the *all* mode - all neurons co-fluctuate, *side* mode - one side dominates the other, *task* mode - the Pro or Anti populations dominate the other,

Sean Bittner
srb2201@columbia.edu

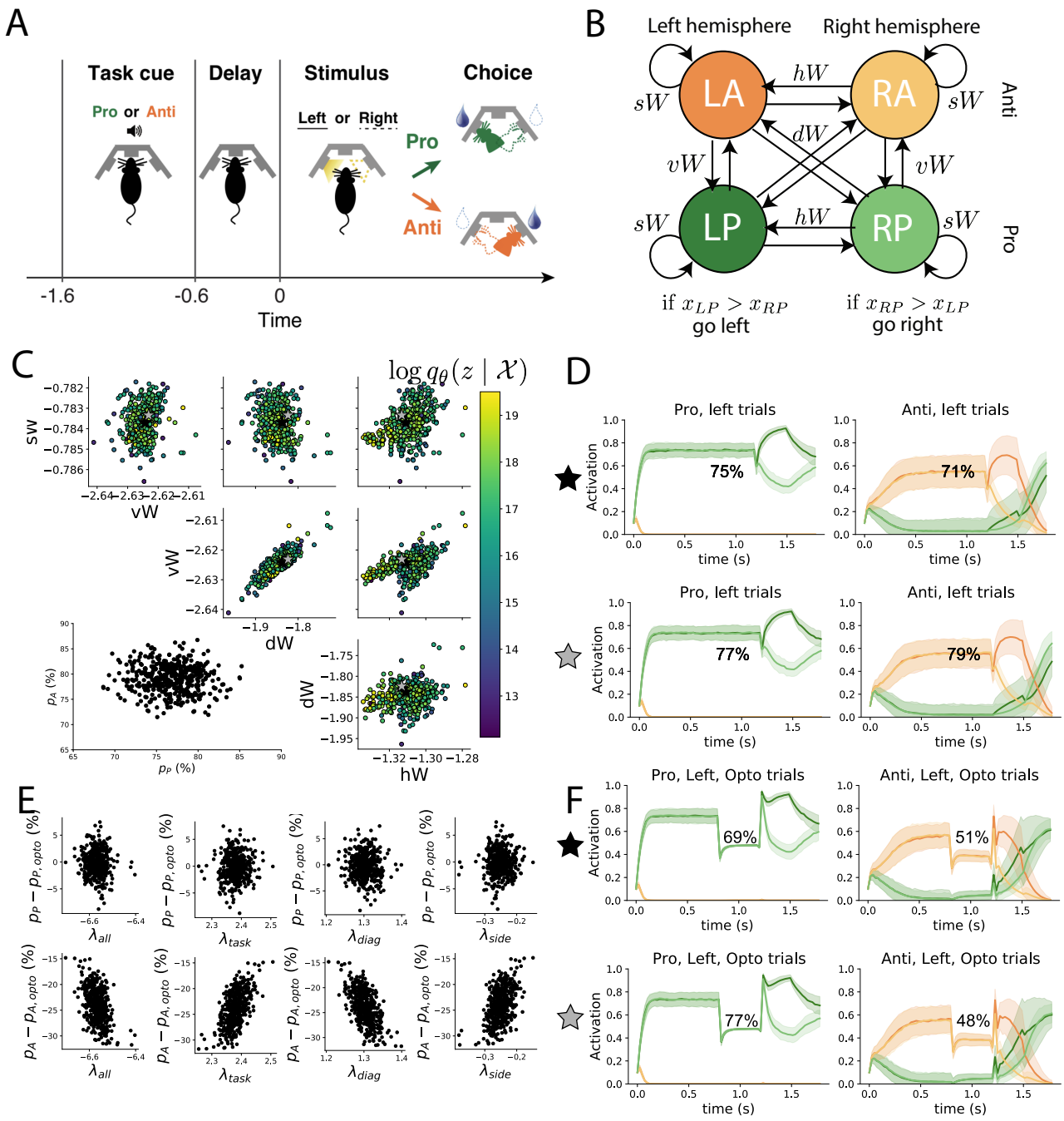


Figure 1: EPI reveals changes in SC [2] connectivity that control task accuracy. A. Rapid task switching behavioral paradigm (see text). B. Model of superior colliculus (SC). Neurons: LP - left pro, RP - right pro, LA - left anti, RA - right anti. Parameters: $sW$ - self, $hW$ - horizontal, $vW$ -vertical, $dW$ - diagonal weights. Subscripts $P$ and $A$ of connectivity weights indicate Pro or Anti populations, and e.g. $vW_{PA}$ is a vertical weight from an Anti to a Pro population. C. The marginal EPI distributions of the Schur eigenvalues at each level of task accuracy. D. Simulations of SC networks with parameterizations indicated by the stars in panel C. Shading shows standard deviations across trials. E. The effect of delay period inactivation on accuracy versus Schur eigenvalues. F. Same as D with delay period inactivation.

and *diag* mode - Pro- and Anti-populations of opposite hemispheres dominate the opposite pair. The corresponding eigenvalues (e.g. $\lambda_{\text{task}}$, which change according to $W$) indicate the degree to which activity along that mode is increased or decreased by $W$.

In agreement with experimental results form Duan et al., we found the optogenetic silencing during the delay period consistently decreased performance in the Anti task by 0-65%, but had no consistent effect on the Pro task (Fig. 1E). For example, the network indicated by the black star suffers a steep drop in accuracy in the Anti task with delay period inactivation (Fig. 1F). Networks resilient to delay period inactivation had greater $\lambda_{\text{task}}$ and $\lambda_{\text{task}}$ and lower $\lambda_{\text{all}}$ and $\lambda_{\text{side}}$ (Fig. 1E).

## 2 Supplementary

$$\mathbf{x}_\alpha = f(\mathbf{u}) = \left(\frac{1}{2}\tanh\left(\frac{u_\alpha - \epsilon}{\zeta}\right) + \frac{1}{2}\right) \tag{3}$$

where $\epsilon = 0.05$ and $\zeta = 0.5$.

The accuracies of $p_P$ and $p_A$ are calculated as

$$p_P(\mathbf{x};\mathbf{z}) = \mathbb{E}_{\mathbf{x}\sim p(\mathbf{x}|\mathbf{z})}\left[\Theta[x_{LP}(t=1.8s) - x_{RP}(t=1.8s)]\right] \tag{4}$$

and

$$p_A(\mathbf{x};\mathbf{z}) = \mathbb{E}_{\mathbf{x}\sim p(\mathbf{x}|\mathbf{z})}\left[\Theta[x_{RP}(t=1.8s) - x_{LP}(t=1.8s)]\right] \tag{5}$$

given that the stimulus is on the left side, where $\Theta$ is the Heaviside step function.

The Heaviside step function is approximated as

$$\Theta(\mathbf{x}) = \text{sigmoid}(\beta\mathbf{x}), \tag{6}$$

where $\beta = 100$.

The system receives five inputs throughout each trial, which has a total length of 1.8s.

$$\mathbf{h}(t) = \mathbf{h}_{\text{constant}} + \mathbf{h}_{\text{P,bias}} + \mathbf{h}_{\text{rule}}(t) + \mathbf{h}_{\text{choice-period}}(t) + \mathbf{h}_{\text{light}}(t). \tag{7}$$

There are rule-based inputs depending on the condition,

$$\mathbf{h}_{\text{constant}} = I_{\text{constant}}[1,1,1,1]^\top \tag{8}$$

$$\mathbf{h}_{\text{P,bias}} = I_{\text{P,rule}}[1,0,1,0]^\top \tag{9}$$

$$\mathbf{h}_{\text{P,rule}}(t) = \begin{cases} I_{\text{P,rule}}[1,0,1,0]^\top, & \text{if } t \le 1.2s \\ 0, & \text{otherwise} \end{cases} \tag{10}$$

$$\mathbf{h}_{\text{A,rule}}(t) = \begin{cases} I_{\text{A,rule}}[0,1,0,1]^\top, & \text{if } t \le 1.2s \\ 0, & \text{otherwise} \end{cases} \tag{11}$$

a choice-period input,

$$\mathbf{h}_{\text{choice}}(t) = \begin{cases} I_{\text{choice}}[1,1,1,1]^\top, & \text{if } t > 1.2s \\ 0, & \text{otherwise} \end{cases} \tag{12}$$

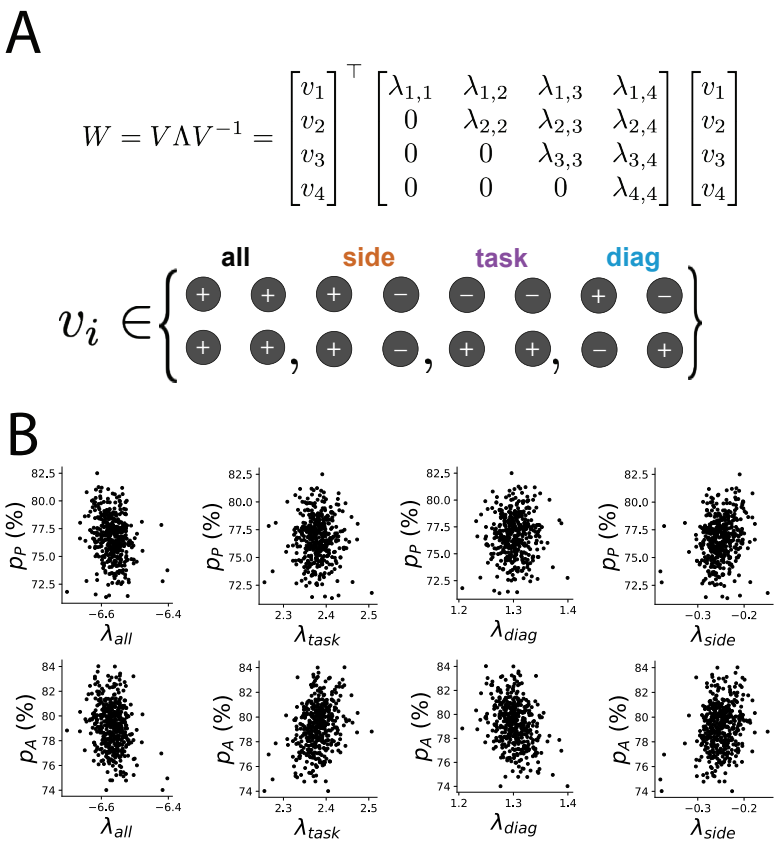


Figure 2: Sentence 1 . A. The Schur decomposition of the weight matrix $W = V\Lambda V^{-1}$ is a unique decomposition with orthogonal $V$ and upper triangular $\Lambda$. Schur modes: $v_{\text{all}}$, $v_{\text{task}}$, $v_{\text{side}}$, and $v_{\text{diag}}$. B. Task accuracy vs. Schur eigenvalue.

and an input to the right or left-side depending on where the light stimulus is delivered.

$$\mathbf{h}_{\text{light}}(t) = \begin{cases} I_{\text{light}}[1,1,0,0]^\top, & \text{if } t > 1.2s \text{ and Left} \\ I_{\text{light}}[0,0,1,1]^\top, & \text{if } t > 1.2s \text{ and Right} \\ 0, & t \leq 1.2s \end{cases}. \tag{13}$$

The input parameterization was fixed to $I_{\text{constant}} = 0.75$, $I_{\text{P,bias}} = 0.5$, $I_{\text{P,rule}} = 0.6$, $I_{\text{A,rule}} = 0.6$, $I_{\text{choice}} = 0.25$, and $I_{\text{light}} = 0.5$.

## References

[1] Chunyu A Duan, Jeffrey C Erlich, and Carlos D Brody. Requirement of prefrontal and midbrain regions for rapid executive control of behavior in the rat. *Neuron*, 86(6):1491–1503, 2015.

[2] Chunyu A Duan, Marino Pagan, Alex T Piet, Charles D Kopec, Athena Akrami, Alexander J Riordan, Jeffrey C Erlich, and Carlos D Brody. Collicular circuits for flexible sensorimotor routing. *bioRxiv*, page 245613, 2018.

Sean Bittner
srb2201@columbia.edu

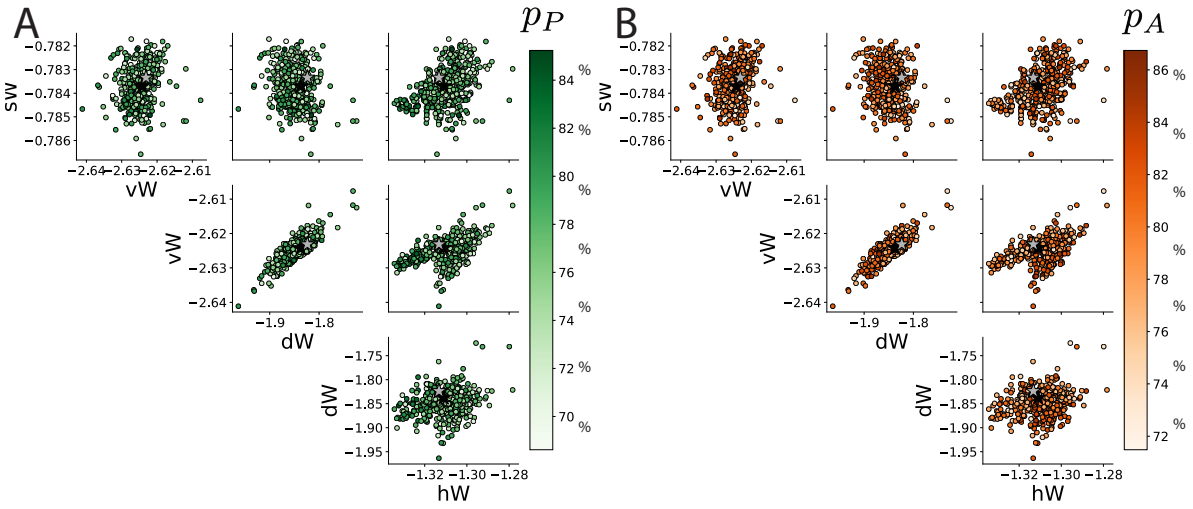


Figure 3: Same as Fig. 1C shaded by Anti task accuracy.